Heliyon 9 (2023) e20149

Contents lists available at ScienceDirect

Heliyon

journal homepage: www.cell.com/heliyon

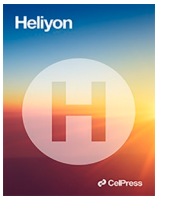

Angong niuhuang wan attenuates LPS-induced acute lung injury by inhibiting PIK3CG/p65/MMP9 signaling in mice based on proteomics

Sen Li [a,1], Jinli Hou [a,1], Qing Wang [b,1], Mei Liu [a], Xingyue Xu [a], Hongjun Yang [a,*], Xianyu Li [a,**]

[a] Beijing Key Laboratory of Traditional Chinese Medicine Basic Research on Prevention and Treatment for Major Diseases, Experimental Research Center, China Academy of Chinese Medical Sciences, Beijing 100700, China
[b] School of Life Sciences, Beijing University of Chinese Medicine, Beijing 100029, China

ARTICLE INFO

Keywords:
Cytokine storm
Angong niuhuang wan
Acute lung injury
Proteomics
Integrated pharmacology
Mechanism research

ABSTRACT

Acute lung injury (ALI) is a serious pulmonary complication that often arises from pneumonia, respiratory tract infections caused by bacteria or viruses, and other factors. It is characterized by acute onset and high mortality. Angong Niuhuang Wan (AGNHW) is a renowned emergency medicine in traditional Chinese medicine, known as the "cool open (febrile disease) three treasures" and regarded as the first of the "three treasures". Previously studies have confirmed that AGNHW has anti-inflammatory effects, improves cerebral circulation, reduces brain edema, and protects vascular endothelium. However, the active components and pharmacological mechanisms of AGNHW in treating ALI remain unclear. In this study, we confirmed that AGNHW can inhibit cytokine storm activity and reduce inflammation induced by LPS in ALI mice. We then analyzed differential proteins using proteomic technology and identified 741 differential proteins. By combining network pharmacological analysis, we deeply discussed the key active components and mechanism of AGNHW in treating ALI. By constructing the interaction network between disease and drug, we identified 21 key active components (such as Quercetin, Kaempferol, and Crocetin) and 25 potential core targets (such as PIK3CG, p65, and MMP9). These candidate targets play an important role in anti-inflammation and immune regulation. Through enrichment analysis of core targets, we found several pathways related to ALI, such as the NF-κB signaling pathway, TNF signaling pathway, and Toll-like receptor signaling pathway. This indicates that AGNHW plays a therapeutic role in ALI through multi-components, multi-targets, and multi-pathways.

1. Introduction

Acute lung injury (ALI) is a condition characterized by acute hypoxemia and lung parenchymal cell injury, often progressing to the

* Corresponding author.
** Corresponding author.
E-mail addresses: lisen0110@163.com (S. Li), 1006223205@qq.com (J. Hou), phd_qingw@foxmail.com (Q. Wang), LM1692276021@163.com (M. Liu), xingyue5125@126.com (X. Xu), hjyang@icmm.ac.cn (H. Yang), lixianyu@merc.ac.cn (X. Li).
[1] These authors contributed equally to this work.

https://doi.org/10.1016/j.heliyon.2023.e20149
Received 5 July 2023; Received in revised form 18 August 2023; Accepted 13 September 2023
Available online 14 September 2023

severe stage of acute respiratory distress syndrome (ARDS) [1]. ALI is commonly caused by severe infection and an uncontrolled systemic inflammatory reaction, known as the cytokine storm. The condition can occur in critical cases such as acute pancreatitis, sepsis, and novel coronavirus, as well as influenza A (H1N1, H5N1, and H7N9) [2]. Unfortunately, there is still a lack of satisfactory therapeutic drugs for ALI, and the use of glucocorticoids has been widely questioned. Despite the use of comprehensive treatment measures, such as mechanical ventilation and extracorporeal membrane oxygenation, the mortality rate remains as high as 40%, making ALI a difficult point in critical care medicine [3,4]. Traditional Chinese Medicine (TCM) has been used for thousands of years in the treatment of various illnesses, including ALI, which has been shown to have several advantages in the treatment of ALI [5]. Firstly, TCM takes a holistic approach to treatment and focuses on restoring balance and harmony within the body. This approach can help to address the underlying causes of ALI and improve overall health and well-being. Secondly, many TCM herbs have anti-inflammatory and antioxidant properties, which could help to reduce inflammation in the lungs and protect against further damage. Thirdly, TCM can be tailored to the individual patient and their specific symptoms and needs. This personalized approach can help to ensure that the treatment is effective and well-tolerated. Finally, TCM is generally considered safe and has few side effects compared to Western medications. This makes it a viable option for patients who may not be able to tolerate or benefit from conventional treatments. As such, it has the potential to be an effective and complementary therapy for ALI [6,7].

Angong Niuhuang Wan (AGNHW) is a TCM consisting of 11 components, including Bovis Calculus Artifactus (NH), Buffalo Horn (SNJ), Moschus (SX), Pearl (ZZ), Cinnabaris (ZS), Realgar (XH), Coptidis Rhizoma (HL), Scutellariae Radix (HQ), Gardeniae Fructus (ZHIZ), Curcumae Radix (YJ), and Borneolum Syntheticum (BP) [8]. It is regarded as the first of the "three treasures" of "cooling and opening" and is derived from the book "Differentiation of Febrile Diseases" by Wu Jutong, a renowned epidemiologist of the Qing Dynasty [9]. AGNHW possesses a range of functions such as clearing heat and detoxifying, opening, and awakening the mind, and treating the syndrome of heat entering the pericardium, high fever, irritability, and delirium [10]. It is an essential medicine for emergency treatment of critical illness in Traditional Chinese medicine. Modern pharmacological studies have confirmed that AGNHW has been shown to inhibit inflammatory responses by reducing the expression levels of IL-1β, TNF-α, IL-13, COX-2, MMP2, MMP9, CCL2, and CCR2 receptor [8,11,12]. In addition to its anti-inflammatory effects, AGNHW has been shown to have a therapeutic effect on ALI [13]. Studies have demonstrated that the AGNHW can reduce lung injury by inhibiting oxidative stress and cell apoptosis, which are common pathological mechanisms underlying ALI. However, the active components and molecular mechanisms in AGNHW, as well as appropriate methods for treating ALI, are still unclear. Therefore, it is crucial to thoroughly investigate AGNHW's mechanism of action for the treatment of ALI.

In the current study, the mouse ALI model was constructed by lipopolysaccharide (LPS) induction, and the active components and potential pharmacological mechanism of AGNHW in the treatment of ALI were studied from the perspective of cytokine storm by using the method of proteomics and integrated pharmacological analysis. This study combines the whole blood proteomics analysis, target prediction and network construction and analysis, comprehensively and systematically reflects the expression of protein and potential active components in vivo, and seeks potential material basis to provide reference for enriching biological mechanism research and clinical application.

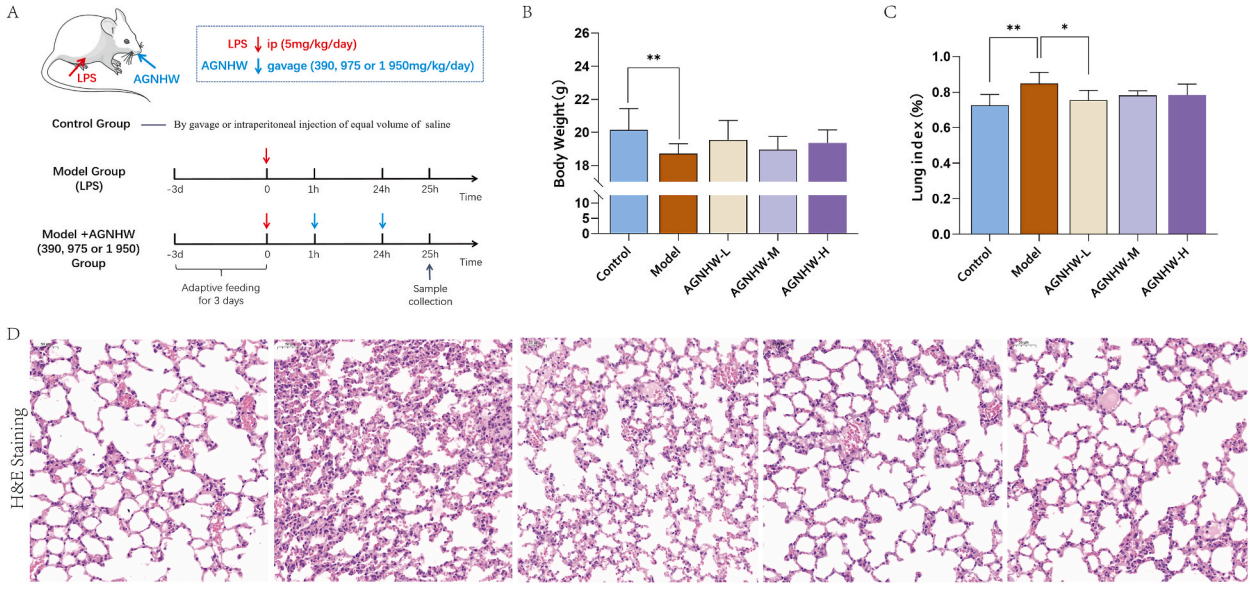

Fig. 1. Comprehensive evaluation index of protective effect of AGNHW on LPS-induced ALI mice. (A) Animal Experiment Protocols. (B) Effect of AGNHW on body weight of ALI model mice. (C) Effect of AGNHW on lung index in ALI model mice. (D) Effects of AGNHW on lung histopathological injury (× 20) by H&E staining. *$P < 0.05$, **$P < 0.01$, ***$P < 0.001$.

2. Materials and methods

2.1. Chemicals and materials

AGNHW was supplied by Zhangzhou Pianzihuang Pharmaceutical Co., Ltd (Zhangzhou, China). Lipopolysaccharide (LPS) was purchased from Biped Sigma (Cat. No. 1128B031, Solarbio, Beijing, China).

2.2. Animals and experimental design

Healthy male Balb/c mice with a SPF grade and weighing between 19.0 - 22.0 g were procured from the Department of Experimental Animal Science at Peking University Medical Department (Beijing, China) with the project identification code 20210013. All animal experiments were permited by the Experimental Animal Ethics Committee of the Experimental Research Center, China Academy of Chinese Medical Sciences (Beijing, China), (approval ID: ERCCACMS21-2208-03). Upon arrival, the animals were housed in a standard laboratory environment and provided free access to food and water. The experiment commenced after the animals adapted to the environment for three days (Fig. 1A).

To prepare for administration, AGNHW was ground and dissolved in normal saline using a mortar to form suspensions of 39.0 mg/mL, 97.5 mg/mL, and 195.0 mg/mL.

The mice were randomly divided into five groups based on their body weight: control, model, and low, medium, and high doses of AGNHW groups (n = 10 per group). To induce ALI in mice, LPS at 5 mg/kg [14], which was soluble in normal saline, was administered intraperitoneally once. As a normal control group, 10 healthy mice were injected intraperitoneally with the equivalent volume of normal saline. One hour after LPS administration, the diarrhea of the mice was observed to confirm the success of the model. Following model confirmation, the corresponding doses of AGNHW were administered to the appropriate groups. The low, medium, and high doses of AGNHW were 390 mg/kg, 975 mg/kg, and 1950 mg/kg BW/day, respectively. The control and model groups were given the same amount of 0.9% NaCl. All groups underwent intragastric administration twice, with a 24 h interval between doses. The condition and body weight changes of the mice were recorded during this period.

One hour after the last administration, blood samples were collected from the eyes of the mice. The blood was collected in sterile tubes and permitted to coagulate at room temperature for an hour. Subsequently, the whole blood was stored at −80 °C for future analysis.

2.3. Lung index and spleen index of mice

Following blood collection, the mice were euthanized, and their lungs and spleens were dissected from each group. The surface mucosal tissue of the organs was meticulously separated and removed using tweezers, and the surface was blotted with filter paper. The weight of the mass was determined using an analytical electronic balance, and the organ index of each tissue was calculated. Weigh the organ weight of each mouse (g), organ index = organ weight/mouse body weight × 100% [15].

2.4. Histopathological evaluation of lung and spleen

The lung tissues were extracted and placed in 4% formalin for 72 h at 4 °C. To examine the histopathological changes in the lungs, sections from paraffin-embedded tissues were stained with hematoxylin and eosin and viewed under a light microscope (Olympus, BX51, Japan).

2.5. Proteomic analysis

After the pharmacological experiments, the eyeballs of mice were removed, and fresh blood was collected and placed in anticoagulant tubes. The samples were gently inverted 2–3 times to ensure thorough mixing and obtain whole blood specimens.

From the obtained whole blood, a 100 μl sample was incubated at room temperature with 400 μl of binding buffer (50 mM Tris, 10 mM EDTA) and 1 mg magnetic polystyrene microspheres (1 μm in diameter). Following magnetic separation, the supernatant was discarded. To clean the bottom magnetic bead precipitation, 1 ml of cleaning buffer (50 mM Tris, 10 mM EDTA) was added and vortexed for 5 min. The remaining solution was centrifuged at 4 °C and 1300 g for 10 min in order to obtain supernatant and observed any hemolysis in the sample. Subsequently, 1 ml washing buffer was added for two washes. Protein electrophoresis buffer was then added to the final binding protein within the magnetic bead precipitation, and boiled for 5 min. The supernatant was subjected to SDS-PAGE electrophoresis for detection.

Furthermore, in the parallel preparation of magnetic bead precipitation, tris (2-carboxyethyl) phosphine, chloroacetamide (an alkylation reagent), and Tris-HCl buffer were combined and allowed to react at 95 °C for 10 min. After cooling to room temperature, 1.5 μg of trypsin was added and the mixture was hydrolyzed at 37 °C for 3 h. Add a formic acid solution with a final concentration of 1%. The sample was centrifuged at 12,000g for 5 min, and the supernatant was then centrifuged in a pre-activated SDB desalting column. This process resulted in the absorption of peptides obtained after enzymolysis onto the SDB column. The SDB column was washed, and the desorbed purified peptide solution was obtained. The purified peptide segments were freeze-dried and stored at −20 °C. Before analysis, the samples were reconstituted with injection buffer and subjected to DIA data acquisition using Nano-LC-MS/MS. Finally, the Spectronaut software was used for data analysis to obtain protein qualitative and quantitative results [16,17].

2.6. Network pharmacological analysis of AGNHW in the treatment of ALI

The Traditional Chinese Medicine Systems Pharmacology Database and Analysis Platform (TCMSP, http://tcmspw.com/tcmsp.php) [18] was utilized to identify the chemical constituents of 11 Traditional Chinese Medicines screening process for active components in AGNHW relied on an oral drug concentration (OB) $\geq$ 30% and drug-like drugs (DL) $\geq$ 0.18, yielding a total of 60 effective chemical components after elimination of duplicates (Supplementary Table S1). Based on the AGNHW component collection results, a research platform grounded on the Integrative Pharmacology-based Research Platform of Traditional Chinese Medicine (TCMIP V2.0, http://www.tcmip.cn/TCMIP/index.php) [19,20] was implemented. The fundamental principle of target prediction is to utilize MedChem Studio (version 3.0) software to detect the structural similarity between the two-dimensional structure of chemical components in DrugBank and approved certified drugs, and use the Tanimoto coefficient to score their similarities. When the similarity score is $\geq$ 0.8 (medium-high similarity), the potential targets of AGNHW chemical composition can be predicted. In total, 434 potential chemical composition targets were identified (Supplementary Table S2). The compound-target network was then constructed using Cytoscape software (version 3.7.1, Boston, MA, USA).

By utilizing "Acute lung injury" as the keyword, disease target genes related to ALI were gathered through OMIM (https://omim.org/) and GeneCards (http://www.genecards.org) disease target databases. After removing duplicates, a total of 1895 disease targets were collected (Supplementary Table S3). Next, the Venn diagram was used to analyze the chemical composition targets of AGNHW along with the related targets of ALI, yielding 200 potential targets (Supplementary Table S4). The intersection of the 200 protein targets predicted by network pharmacology and the 741 targets obtained by proteomics was obtained (Supplementary Table S5), followed by introducing the information of "Traditional Chinese Medicine-compound-target" corresponding to the 25 coincident targets (Supplementary Table S6) in the experiment into Cytoscape software for visualization and network topology analysis to construct a protein interaction network.

2.7. GO analysis and KEGG analysis

The functional enrichment of effective proteins was analyzed via Gene ontology (GO) function and Kyoto Encyclopedia of Genes and Genomes (KEGG) pathway enrichment analysis. To achieve this, effective targets obtained from the above analysis, differential proteins obtained from Proteomics analysis and core targets shared by differential proteins and network pharmacology, were input into the DAVID database (https://david-d.ncifcrf.gov/, version 6.8) for GO and KEGG enrichment analysis in order to further investigate the specific function of the protein and the involved pathway process.

2.8. Quantitative real-time reverse transcriptase polymerase chain reaction (qPCR)

Total RNA was extracted from lung tissue using the FastPure Cell/Tissue Total RNA Isolation Kit V2 (Vazyme, Nanjing, China). The PCR reaction method is as follows: Stage 1: Pre-denaturation, accomplished one cycle at 95 °C for 30 s; Stage 2: The PCR reaction was conducted for 40 cycles consisting of 10 s at 95 °C and 30 s at 60 °C; Stage 3: Melting curve was performed by heating the cycle from 60°C to 95 °C/s at a rate of 0.05 °C/s. The relative expression levels of IL-1β, IL-6, TNF-α, TLR-4, iNOS, IFN-γ, PIK3CG, p65, and MMP9 were measured using the $2^{-\Delta\Delta Ct}$ method, with GAPDH serving as the internal control. All qPCR experiments were replicated three times. Table 1 presents the primer sequences utilized in this study.

Table 1
Primers used in this study.

Gene primer name	Primer sequence (5′-3′)
GAPDH_F	TGTTTCCTCGTCCCGTAGA
GAPDH_R	ATCTCCACTTTGCCACTGC
IL-6_F	ACAGAAGGAGTGGCTAAGGA
IL-6_R	AGGCATAACGCACTAGGTTT
TNF-α_F	CGCTGAGGTCAATCTGC
TNF-α_R	GGCTGGGTAGAGAATGGA
IL-1β_F	AGTTGACGGACCCCAAA
IL-1β_R	TCTTGTTGATGTGCTGCTG
iNOS_F	GTTCTCAGCCCAACAATACAAGA
iNOS_R	GTGGACGGGTCGATGTCAC
TLR-4_F	ATGGCATGGCTTACACCACC
TLR-4_R	GAGGCCAATTTTGTCTCCACA
IFN-γ_F	ATGAACGCTACACACTGCATC
IFN-γ_R	CCATCCTTTTGCCAGTTCCTC
MMP9_F	CTGGACAGCCAGACACTAAAG
MMP9_R	CTCGCGGCAAGTCTTCAGAG
p65_F	AGGCTTCTGGGCCTTATGTG
p65_R	TGCTTCTCTCGCCAGGAATAC
PIK3CG_F	CACTGGAGTCACCGGCTAC
PIK3CG_R	GACACTGTGAACACACTCTCG

2.9. Western blot

Mouse lung tissue was lysed with RIPA cleavage buffer and supplemented with protease inhibitor and phosphatase inhibitor (Solarbio, Beijing, China). The protein concentration was quantified using a BCA protein analysis kit (Pierce, California, USA). Subsequently, 20 μg of protein was resolved by 10% sodium dodecyl sulfate-polyacrylamide gel electrophoresis (SDS-PAGE) and transferred onto a polyvinylidene fluoride (PVDF) membrane (Milipole, Massachusetts). The membrane was then blocked overnight at 4 °C using 5% skim milk. Subsequently, the membrane was probed with anti-P65 (Cat. No.3033T, 1:1,000, Cell Signaling Technology, America), P-p65 (Cat. No.3033T, 1:1,000, Cell Signaling Technology, America), PIK3CG (Cat. No.MA01517, 1:1,000, Boster, Wuhan, China), or MMP9 (Cat. No.BA2202, 1:1,000, Boster, Wuhan, China) primary antibodies overnight at 4 °C. The internal control, GAPDH (Cat. No.60004-1-Ig, 1:50,000, Proteintech, Wuhan, China), was included alongside the other primary antibodies. The membrane was subsequently incubated with the secondary antibody at room temperature for 1 h, and protein bands were detected using an enhanced chemiluminescence agent (Milipole, Massachusetts, USA).

2.10. Statistical analysis

Image J (Bio-Rad, Hercules, CA, USA) was used for quantitative analysis of target bands on Western blots. Histogram and statistical analysis were carried out in GraphPad Prism (GraphPad Prism 8.0, San Diego, CA, USA). Results were shown as mean ± standard deviation (SD). ANOVA followed by Tukey's post hoc test was used to compare mean values of multiple groups. The significant difference was set at $P < 0.05$, $P < 0.01$, $P < 0.001$.

3. Results

3.1. Effect of AGNHW on body weight of ALI model mice

As shown in Fig. 1B, the body weight of the ALI model mice (model group) was significantly decreased in comparison to that of the normal mice (control group) ($P < 0.05$). However, the AGNHW low, medium, and high dose groups exhibited an upward trend compared to that of the model group, although the differences were not statistically significant.

3.2. Effect of AGNHW on lung index in ALI model mice

As shown in Fig. 1C, the lung index of the model group was significantly increased compared to the control group ($P < 0.05$).

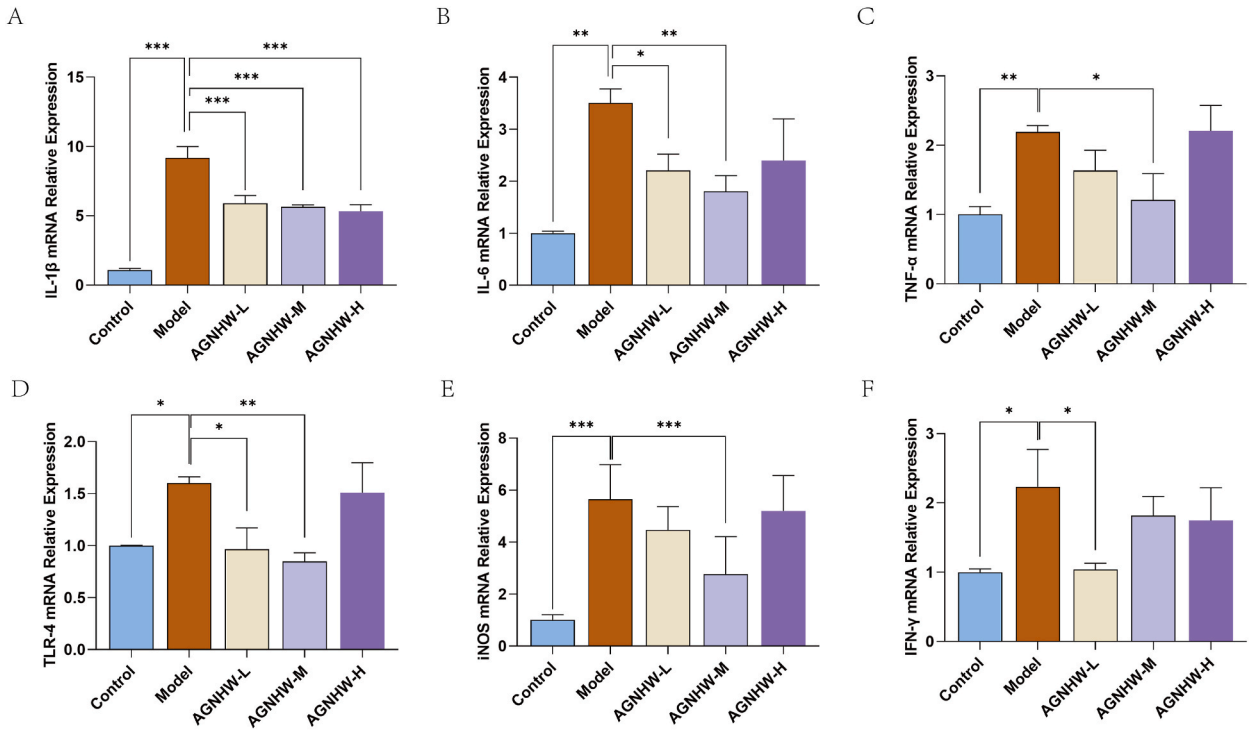

Fig. 2. Effect of AGNHW on inflammatory factors in ALI model mice. The mRNA expression of (A) IL-1β, (B) IL-6, (C) TNF-α, (D) TLR-4, (E) iNOS, (F) IFN-γ. *$P < 0.05$, **$P < 0.01$, ***$P < 0.001$.

However, the lung index of the low dose AGNHW group was significantly lower than that of the model group ($P < 0.05$).

3.3. Effect of AGNHW on lung tissue histopathology

As shown in Fig. 1D, the lung tissue structure of the blank group was normal, with clear alveoli and relatively uniform size. There was no observable thickening of alveolar walls, no proliferation of epithelial cells, and no infiltration of inflammatory cells. In contrast, the lung tissue structure of the model group was abnormal, exhibiting a significant number of atrophic and collapsed alveoli, proliferating epithelial cells, thickening of the alveolar wall, and infiltration of inflammatory cells. Following administration of AGNHW, the degree of lung tissue injury was slightly improved in the low dose group compared to that of the model group. However, the middle dose group exhibited more substantial improvement. Although the high dose group exhibited the most significant reduction in inflammatory cell infiltration, the lung tissue structure remained visibly damaged.

3.4. Effect of AGNHW on inflammatory factors in ALI model mice

As shown in Fig. 2 (A-F), the mRNA expression levels of IL-1β, IL-6, TNF-α, TLR-4, iNOS, and IFN-γ in the lung tissue of the model group were significantly higher than those of the control group ($P < 0.05$). However, in comparison to the model group, the levels of the aforementioned antiinflammatory factors were significantly lower in the lung tissue of the AGNHW group.

3.5. Proteomic analysis of ALI mice treated with AGNHW

A total of 6110 proteins were identified through mass spectrometry and protein data retrieval with 5526 of them being quantifiable. The quantifiable data underwent linear function normalization, and then identified differential proteins. Statistical analysis of the protein quantitative differences between groups (controls vs. ALI mouse model) revealed that 292 proteins were up-regulated, and 449 proteins were down-regulated (Fig. 3A). Significantly altered proteins were those with fold changes >1.2 ($P < 0.05$). Among these differentially expressed proteins (DEPs), PIK3CG, p65, and MMP9 are the most significantly expressed, therefore these proteins serve

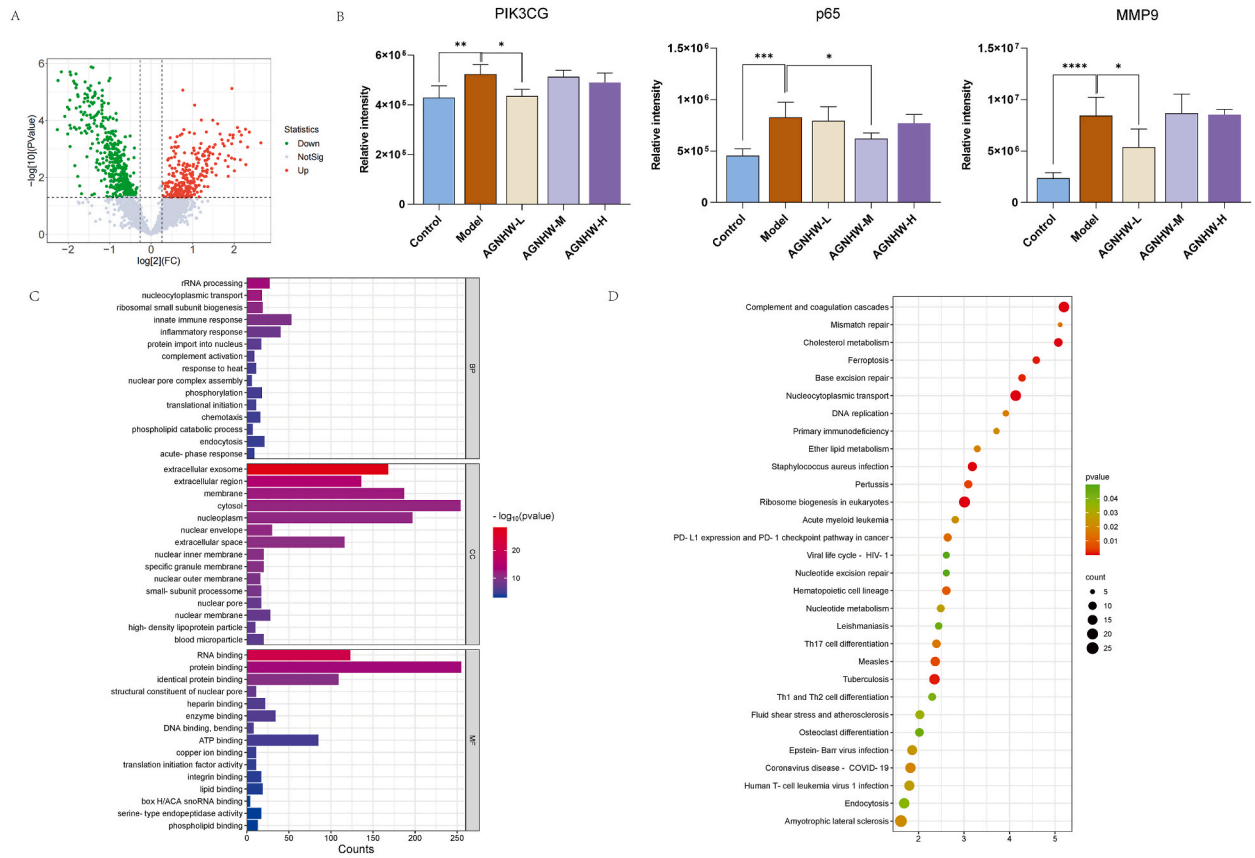

Fig. 3. Proteomic analysis of model group and control group (n = 6). (A) Volcano plot of the model group and the control group proteins. (B) Expression level change of the 3 selected proteins with significant differences between the model group and the control group. (C) GO enrichment analysis of 741 differential proteins. (D) KEGG pathway analysis of 741 differential proteins. *$P < 0.05$, **$P < 0.01$, ***$P < 0.001$.

as potential targets for further research (Fig. 3B). The DEPs were subject to GO functional enrichment analysis from three aspects: biological process (BP), molecular function (MF), and cellular components (CC). The top 15 functions were selected for visualized analysis. At the BP level, the differentially expressed proteins were mainly involved in BP such as innate immune response, inflammatory response, protein import into nucleus, complement activation, etc. From the perspective of MF, the differentially expressed proteins primarily performed molecular regulatory functions, including RNA binding, ATP binding, protein binding, etc. In terms of CC, most of the differentially expressed proteins were derived from the extracellular exosome, extracellular region and Membrane (Fig. 3C).

The identified DEPs were used to carry out KEGG pathway enrichment analysis, and the top 30 pathways were plotted. The KEGG pathway annotation results showed that the differentially expressed proteins were primarily involved in Complement and coagulation cascades, Nucleocytoplasmic transport, Cholesterol metabolism, Staphylococcus aureus infection, Ferroptosis, and other related signaling pathways (Fig. 3D). The KEGG pathway enrichment analysis demonstrated that the differentially expressed proteins were primarily concentrated in critical pathways such as inflammation and immune regulation.

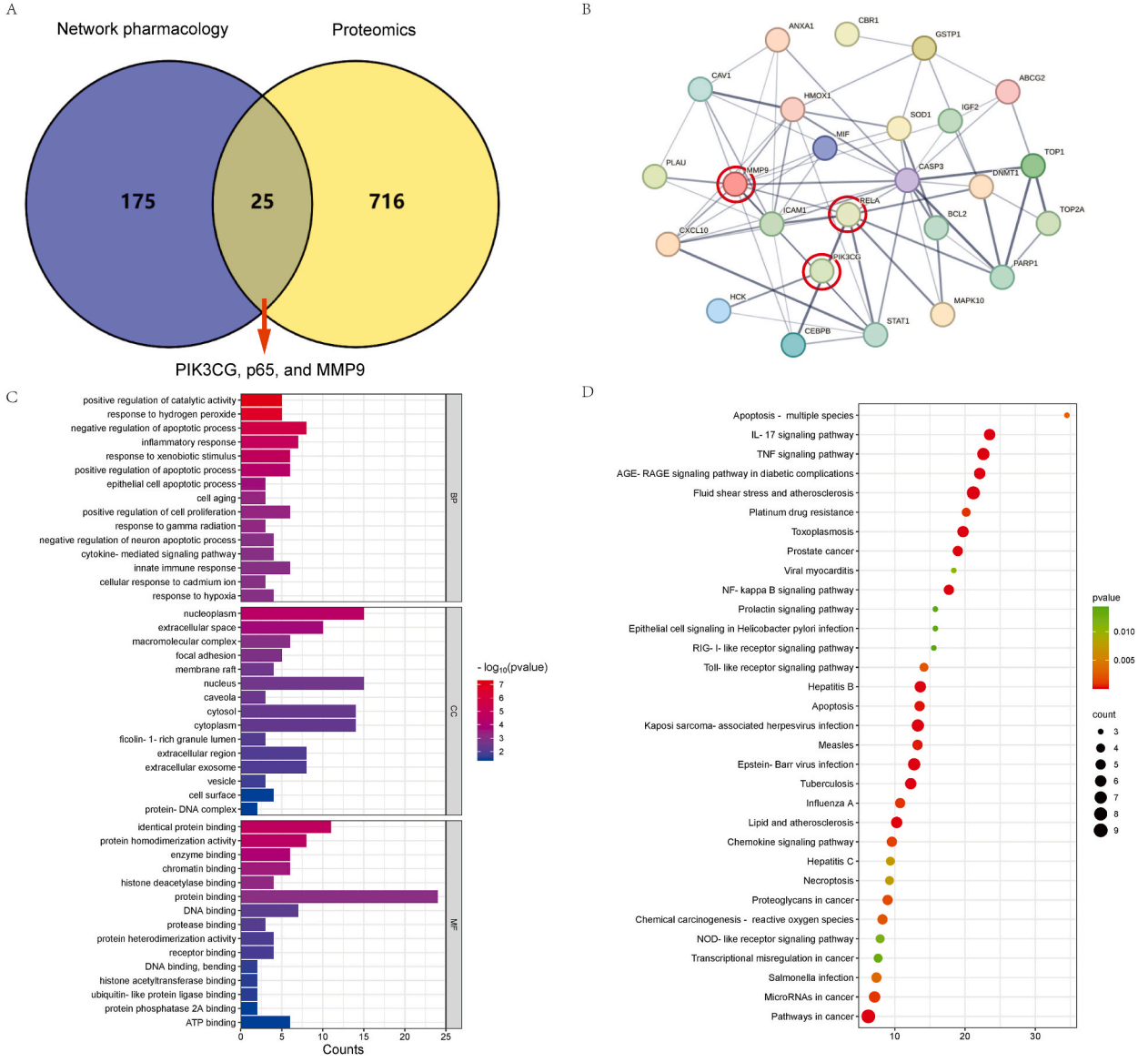

Fig. 4. Combination analysis of proteomics and network pharmacology. (A) Venny analysis of differential proteins and core targets of network pharmacology. (B) PPI analysis of coincidence target. (C) GO enrichment analysis of coincidence target. (D) KEGG pathway analysis of coincidence target.

3.6. Integrated analysis of proteomics and network pharmacology

Based on information from OMIM and GeneCards disease target database, a total of 1895 genes associated with ALI were collected and can be found in Supplementary Table S3. In order to investigate the potential targets of AGNHW on ALI, we analyzed the Venny 2.1.0 database (https://bioinfogp.cnb.csic.es/tools/venny/) and identified 200 common targets. These common targets serve as a foundation for further research. Supplementary Table S4 offers a detailed overview of the shared targets between AGNHW targets and ALI-related genes.

Using network pharmacology analysis, we identified 25 common targets between the disease and AGNHW, including notable targets such as RELA (p65), PIK3CG, and MMP9 (Fig. 4A). The Protein-Protein Interaction (PPI) network for these 25 common targets was constructed through the String database (https://cn.string-db.org/), demonstrating a polycentric interaction network that emphasizes the importance of core target proteins with a higher number of node connections (Fig. 4B). Additionally, analysis of the GO function of the 25 common protein targets revealed their involvement in a variety of BP, including response to hydrogen peroxide, negative regulation of apoptotic process, and inflammatory response. Cellular components were primarily distributed in the nucleoplasm, extracellular space, macromolecular complex, and focal adhesion, while molecular functions included enzyme binding, ATP binding, and protein binding (Fig. 4C). The 25 common targets mainly participate in pathways such as NF-κB signaling, TNF signaling, and Toll-like receptor signaling (Fig. 4D). Finally, we used Cytoscape software to visualize the relationships among TCM formulas, herbs, chemical compounds, targets, pathways, and pharmacological effects (Fig. 5). The results indicate that regulating these 25 targets requires the use of 7 kinds of TCM and 21 chemical compounds. Based on literature review, we identified p65, PIK3CG, and MMP9 as the main ALI-related targets. The network diagram revealed that p65 was primarily regulated by Crocetin and Quercetin. Thus, the NF-κB signaling pathway, TNF signaling pathway, and Toll-like receptor signaling pathway can be directly or indirectly regulated to exert their anti-inflammatory effects. PIK3CG was mainly influenced by AGNHW Isoimperatorin, Isokaempferide,

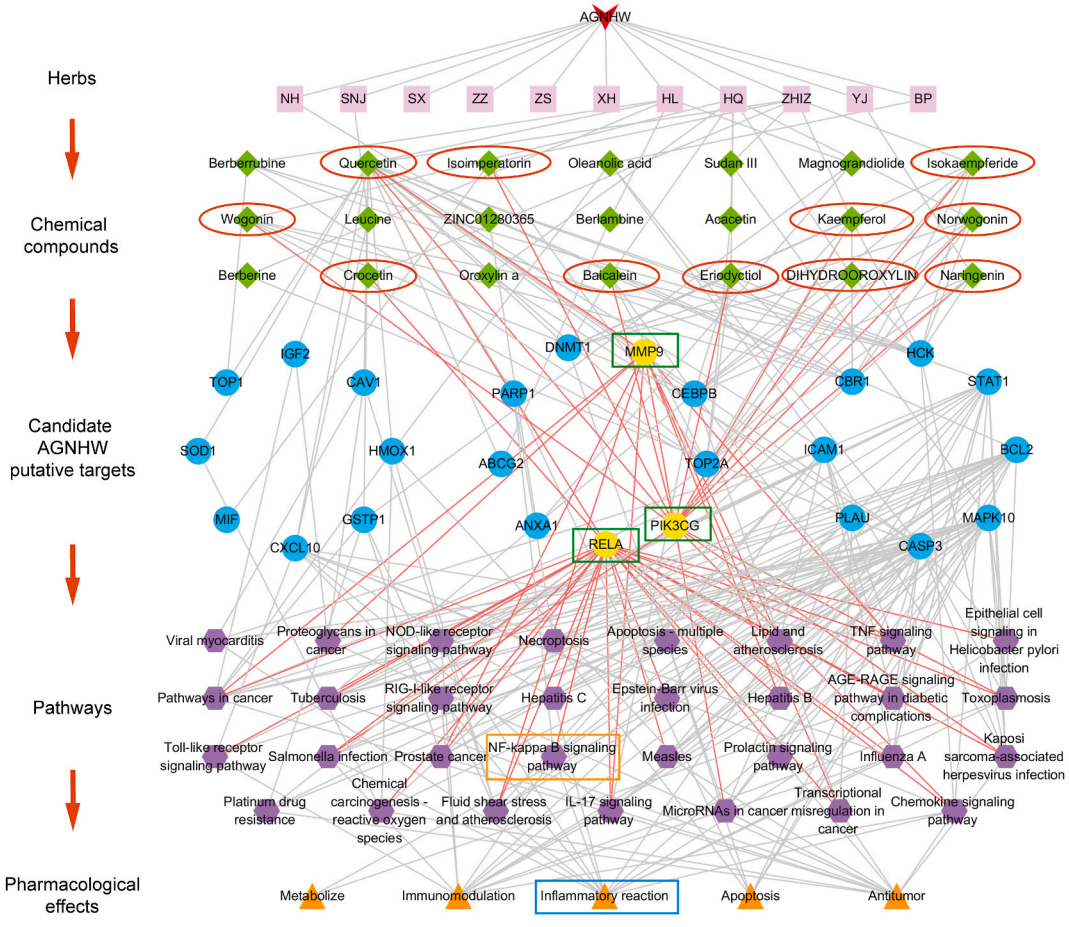

Fig. 5. Explain the correlation among the chemical components, candidate targets, involved pathways and corresponding pharmacological effects of AGNHW. The red node represents the AGNHW prescription; the pink target represents the Traditional Chinese Medicine contained in the AGNHW prescription; the green node represents the chemical components contained in AGNHW; the blue node refers to the candidate target of AGNHW; the yellow node refers to the known ALI-related genes; the purple node refers to the regulatory pathway of the candidate target of AGNHW; and the orange node refers to the corresponding pharmacological action of the main pathway of AGNHW in the treatment of ALI.

Kaempferol, Quercetin, Naringenin, Wogonin, Baicalein, Eriodyctiol, DIHYDROOROXYLIN, Norwogonin, and other chemical compounds, which then regulate TNF signaling pathway and Chemokine signaling pathway to exert their anti-inflammatory effects directly or indirectly. MMP9 was predominantly regulated by Quercetin, which then regulated the NF-κB signaling pathway, TNF signaling pathway, and Fluid shear stress and atherosclerosis signaling pathways to exert its anti-inflammatory effects directly.

3.7. Expression of PIK3CG, p65 and MMP9 mRNA

To confirm the validity of our combined analysis using proteomics and network pharmacology, we conducted qPCR to assess the expression levels of key genes, including PIK3CG, p65, and MMP9, which are primarily associated with the NF-κB signaling pathway. The expression levels of these genes were significantly higher in the lung tissue of ALI model mice compared to the control group. However, after treatment with AGNHW, the expression levels of PIK3CG, p65, and MMP9 were significantly reduced compared to the model group ($P < 0.05$, Fig. 6A–C).

3.8. Expression of PIK3CG, p65 and MMP9 proteins

To further validate the expression of differential protein, we used Western blotting to measure the levels of PIK3CG, p65, P-p65 and MMP9 in lung tissue (Fig. 6D–K). Our results showed that the expression of these proteins was markedly increased in the model group compared to the control group. However, treatment with AGNHW significantly reduced the levels of PIK3CG, p65, P-p65, and MMP9 compared to the model group. These findings were consistent with our PCR analysis results, confirming the ability of AGNHW to regulate the expression of these key proteins.

4. Discussion

Acute lung injury (ALI) is a disease characterized by damage to alveolar epithelial and capillary endothelial cells, the triggering of inflammatory factors, and the accumulation of neutrophils due to factors apart from cardiogenic factors like severe infection, shock, and trauma [21]. Despite progress made in understanding the etiology and pathology of ALI, treatment options remain limited, with a clinical mortality rate of around 50%. Aside from mechanical ventilation strategies and life support treatment, researchers urgently need to explore the pathogenesis and treatment of ALI, ultimately restoring the body to normal homeostasis [22]. Cytokine storm is a broad term encompassing various immune malfunction diseases. If not treated properly, it may result in multiple organ failure [2,23].

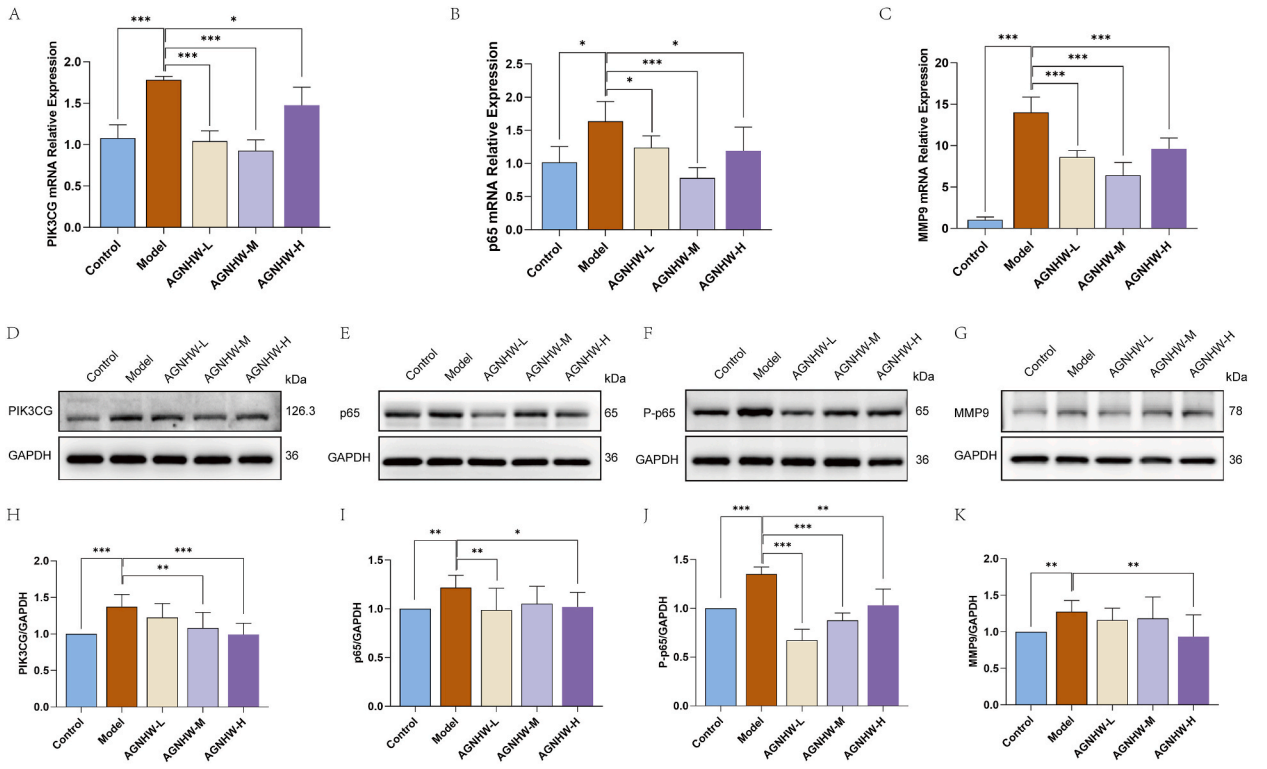

Fig. 6. The results of mRNA and Western blotting of the three key targets (n = 3). (A–C) The mRNA expression of PIK3CG, p65 and MMP9. (D–K) The proteins expression of PIK3CG, p65, P-p65 and MMP9. *$P < 0.05$, **$P < 0.01$, ***$P < 0.001$.

Studies suggest that when ALI occurs, the immune system becomes overactivated, triggering cytokine storms that release abundant IL-6, TNF-α, and IFN-γ. However, the complexity of cytokines poses certain limitations to the use of specific cytokine blockers [24]. TCM with its multi-target and personalized syndrome differentiation and treatment features, particularly its unique advantages in intervening in "inflammatory storms" in COVID-19, can offer critical insights into inflammatory regulation [25,26]. Cytokine storms present no apparent symptoms before onset and are difficult to treat once they take hold, often with severe consequences. Therefore, prevention and treatment should primarily focus on early intervention. TCM with its distinctive advantage in treating before onset and preventing further transmission, can address this issue effectively.

Modern pharmacological studies have demonstrated that AGNHW possesses anti-inflammatory properties, enhances cerebral circulation, reduces brain edema, and protects vascular endothelium, among other effects [27–29]. AGNHW is widely used in clinical practice for the treatment of stroke, cerebral edema, cerebral hemorrhage, sepsis, and other diseases [30]. In this study, we focused on the role of AGNHW in the LPS-induced ALI animal model. Our findings demonstrated that AGNHW effectively improved the body weight and lung index of LPS-induced ALI model mice, exhibiting a strong inhibitory effect on inflammatory factors such as IL-6, TNF-α, and IFN-γ released by cytokine storm. Moreover, AGNHW significantly ameliorated LPS-induced lung tissue injury. Collectively, the experimental data provide evidence that AGNHW exerts a protective effect on LPS-induced ALI.

To elucidate the material basis and molecular mechanism of AGNHW in treating ALI, we conducted a joint analysis using whole blood proteomics and network pharmacology. The KEGG pathway analysis indicated that the identified targets were associated with immune and inflammatory signaling pathways, including the IL-17 signaling pathway, Chemokine signaling pathway, NF-κB signaling pathway, TNF signaling pathway and Toll-like receptor signaling pathway. This suggested that inflammatory signaling pathways were implicated in the onset and progression of ALI. Numerous studies have highlighted the crucial role of PIK3CG in regulating the IκBα/NF-κB signaling pathway and innate immune response, making it a promising therapeutic target for the treatment of LPS-induced ALI [31]. NF-κB is a protein complex functioning in almost all animal cell types and plays a significant role in cellular stress response, cytokine reactions, and immune responses to viral or bacterial antigens, among others. Specifically, LPS from Gram-negative bacteria activates TLR4, ultimately leading to the activation of NF-κB to enter the nucleus and modulate the gene expression related to inflammation and apoptosis [32]. NF-κB also acts as the upstream regulator of MMPs gene and is a key transcription factor that modulates immune and neuroinflammatory responses. Notably, studies have shown that curcumin is an effective treatment for LPS-induced ALI, and its mechanism may involve reducing the expression of MMP2 and MMP9 proteins, which in turn mitigates the aggregation and activation of neutrophils in lung tissue and significantly reduces lung tissue inflammation [33].

Further, network pharmacology analysis identified 21 potentially active key components and 25 potential core targets that may be responsible for the therapeutic effects of AGNHW. Importantly, these 25 core target proteins are well-established candidates for ALI, and research has demonstrated their crucial role in the alleviation and management of ALI symptoms. The core targets were analyzed using GO and KEGG by DAVID to determine their function and associated action pathways. The resulting data were used to draw a multi-level association network diagram using Cytoscape, which shown the relationship between "TCM-key active components-core targets-key pathways-pharmacological actions". This diagram helped to clarify the pharmacological basis and potential molecular mechanism of AGNHW in treating ALI. Studies have found that certain components within AGNHW possess beneficial effects in alleviating the pathological symptoms of ALI. For instance, baicalein can inhibit the inflammatory response mediated by NF-κB and up-

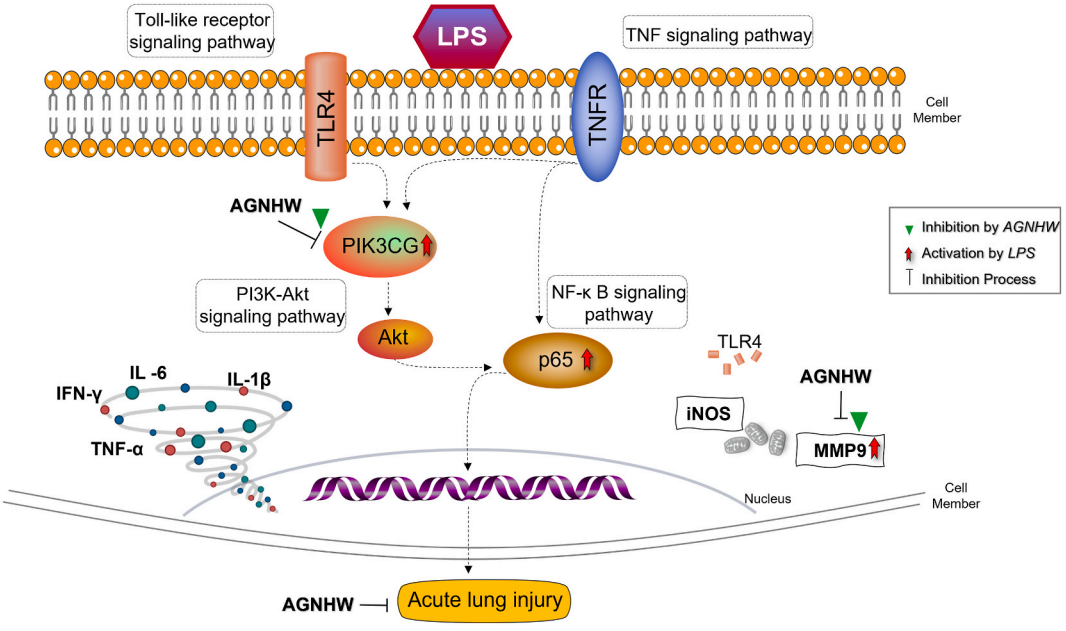

Fig. 7. Schematic illustration of the main pathways of AGNHW in the treatment of LPS-induced ALI.

regulate the Nrf2/HO-1 pathway, thereby alleviating ALI symptoms [34,35]. Quercetin has been found to possess a protective effect against LPS-induced ALI in SD rats. This effect may be attributed to its ability to regulate the NF-κB signaling pathway by down-regulating the expression of NF-κB/p65 and reducing the release of pro-inflammatory factors [36]. Similarly, kaempferol has been shown to exert a protective effect on LPS-induced ALI in mice by inhibiting the mRNA expression of pro-inflammatory cytokines such as NF-κB, IL-1β, and TNF-α [36,37]. Further studies have demonstrated that Crocetin, a carotenoid compound, can effectively reduce inflammation and inhibit the production of reactive oxygen species. The inhibition of the NF-κB signaling pathway by saffron has also been found to be beneficial in alleviating LPS-induced ALI in mice. In a mouse model of LPS-induced ALI, Crocetin significantly reduced the mRNA and protein expression of IL-6 and TNF-α in lung tissue. Additionally, different doses of Crocetin were able to reduce NF-κB activity [38]. Overall, these findings support the potential therapeutic effects of Quercetin, kaempferol, and Crocetin in mitigating the inflammatory response and protecting against LPS-induced ALI.

To verify the accuracy of the proteomics and network pharmacology joint analysis results, we assessed the mRNA and protein expression levels of PIK3CG, p65, and MMP9 in conjunction with existing literature. Results revealed that the LPS-induced ALI model significantly upregulated the expression levels of PIK3CG, p65, and MMP9 in lung tissue, which aligned with previous research [31,32]. This study sheds light on the mechanism underlying the therapeutic effect of AGNHW in the management of ALI (Fig. 7). Results suggested that AGNHW may act through a multi-component, multi-target, and multi-mechanism pathway, highlighting the therapeutic characteristics of traditional Chinese medicine.

5. Conclusion

In conclusion, our study provides fundamental research evidence for the utilization of AGNHW in the treatment of ALI. Our results demonstrate that AGNHW effectively mitigates abnormal body weight, lung index, and inflammatory factor levels in LPS-induced ALI mice. AGNHW appears to exert its therapeutic effects on ALI through various chemical components, such as Quercetin, Kaempferol, and Crocetin, which target immune regulation and inflammation-related biomolecules, including PIK3CG, p65, MMP9, and others. These chemical components modulate several pathways, including the NF-κB, TNF, and Toll-like receptor signaling pathways. Overall, these findings align with existing literature on ALI treatment, highlighting the molecular mechanism of AGNHW in ALI management. Our study employs a combination of proteomics and network pharmacology to analyze the mechanism of AGNHW in the treatment of ALI, reflecting the relationship between macro and micro approaches, virtual computing, and experimental detection. Nonetheless, our study only examines a fraction of the pathway and related targets, and follow-up studies are necessary to validate more targets on the pathway to fully elucidate the mechanism of AGNHW in ALI treatment.

Author contribution statement

Sen Li; Jinli Hou; Qing Wang: Performed the experiments; Analyzed and interpreted the data; Contributed reagents, materials, analysis tools or data; Wrote the paper.

Mei Liu; Xingyue Xu: Contributed reagents, materials, analysis tools or data.

Hongjun Yang; Xianyu Li: Conceived and designed the experiments.

Data availability statement

Data will be made available on request.

Funding

This work was supported by the National Natural Science Foundation of China (82174238, 32000019), China; the grants from the Scientific and technological innovation project of China Academy of Chinese Medical Sciences (CI2021A05032, CI2021B017), China; and the Fundamental Research Funds for the Central Public Welfare Research Institutes (ZZ13-YQ-080, ZZ16-YQ-038, RXRC2022003, JBGS2021003), China.

Declaration of competing interest

The authors declare that they have no known competing financial interests or personal relationships that could have appeared to influence the work reported in this paper.

Appendix A. Supplementary data

Supplementary data to this article can be found online at https://doi.org/10.1016/j.heliyon.2023.e20149.

References

[1] M.E. Long, R.K. Mallampalli, J.C. Horowitz, Pathogenesis of pneumonia and acute lung injury, Clin. Sci. (London, England: 1979) 136 (2022) 747–769.
[2] J.Y. Kang, M.M. Xu, Y. Sun, Z.X. Ding, Y.Y. Wei, D.W. Zhang, Y.G. Wang, J.L. Shen, H.M. Wu, G.H. Fei, Melatonin attenuates LPS-induced pyroptosis in acute lung injury by inhibiting NLRP3-GSDMD pathway via activating Nrf2/HO-1 signaling axis, Int. Immunopharm. 109 (2022), 108782.
[3] S. Shaefi, S.K. Brenner, S. Gupta, B.P. O'Gara, M.L. Krajewski, D.M. Charytan, S. Chaudhry, S.H. Mirza, V. Peev, M. Anderson, A. Bansal, S.S. Hayek, A. Srivastava, K.S. Mathews, T.S. Johns, A. Leonberg-Yoo, A. Green, J. Arunthamakun, K.M. Wille, T. Shaukat, H. Singh, A.J. Admon, M.W. Semler, M. A. Hernán, A.L. Mueller, W. Wang, D.E. Leaf, Extracorporeal membrane oxygenation in patients with severe respiratory failure from COVID-19, Intensive Care Med. 47 (2021) 208–221.
[4] D. Impellizzeri, G. Bruschetta, E. Esposito, S. Cuzzocrea, Emerging drugs for acute lung injury, Expet Opin. Emerg. Drugs. 20 (2015) 75–89.
[5] J. Guo, J. Zhu, Q. Wang, J. Wang, Y. Jia, Comparative efficacy of seven kinds of Chinese medicine injections in acute lung injury and acute respiratory distress syndrome: a network meta-analysis of randomized controlled trials, Front. Pharmacol. 12 (2021), 627751.
[6] G. Deng, H. He, Z. Chen, L. OuYang, X. Xiao, J. Ge, B. Xiang, S. Jiang, S. Cheng, Lianqinjiedu decoction attenuates LPS-induced inflammation and acute lung injury in rats via TLR4/NF-κB pathway, Biome Pharmacother. 96 (2017) 148–152.
[7] Y. Wu, W. Zhu, A. Rouzi, L. Tong, L. Han, J. Song, J. Ding, Y. Yan, M. Li, T. Pan, J. Liu, Q. Wang, Y. Song, J. Shen, J. Zhou, The traditional Chinese patented medicine Qingke Pingchuan granules alleviate acute lung injury by regenerating club cells, Pulm. Circ. 12 (2022), e12138.
[8] Y. Chai, Z. Yin, Q. Fan, Z. Zhang, K. Ye, Y. Xu, W. Xiao, X. Chai, T. Zhu, H. Nie, Protective effects of angong Niuhuang pill on early atherosclerosis in ApoE(-/-) mice by reducing the inflammatory response, evidence-based complementary and alternative medicine, Evid Based Complement Alternat Med. 2019 (2019), 9747212.
[9] H. Zhang, X. Hui, Y. Wang, Y. Wang, X. Lu, Angong Niuhuang Pill ameliorates cerebral ischemia/reperfusion injury in mice partly by restoring gut microbiota dysbiosis, Front. Pharmacol. 13 (2022), 1001422.
[10] H. Chen, Y. Luo, B. Tsoi, B. Gu, S. Qi, J. Shen, Angong Niuhuang Wan reduces hemorrhagic transformation and mortality in ischemic stroke rats with delayed thrombolysis: involvement of peroxynitrite-mediated MMP-9 activation, Chin. Med. 17 (2022) 51.
[11] Q. Fan, Y. Liu, J. Rao, Z. Zhang, W. Xiao, T. Zhu, X. Chai, K. Ye, N. Ning, Z. Yin, Y. Chai, Y. Xu, R. Lan, A. Verkhratsky, H. Nie, Anti-atherosclerosis effect of angong Niuhuang pill via regulating Th17/treg immune balance and inhibiting chronic inflammatory on ApoE(-/-) mice model of early and mid-term atherosclerosis, Front. Pharmacol. 10 (2019) 1584.
[12] F. Zhang, Y. Lu, J. Liu, J. Shi, [Realgar is active ingredient of Angong Niuhuang pill in protection against LPS-induced neuroinflammation], Zhongguo Zhong Yao Za Zhi. 35 (2010) 3333–3338.
[13] W. Zhuang, Z. Fan, Y. Chu, H. Wang, Y. Yang, L. Wu, N. Sun, G. Sun, Y. Shen, X. Lin, G. Guo, S. Xi, Chinese patent medicines in the treatment of coronavirus disease 2019 (COVID-19) in China, Front. Pharmacol. 11 (2020) 1066.
[14] X. Zhang, C. Li, J. Li, Y. Xu, S. Guan, M. Zhao, Protective effects of protocatechuic acid on acute lung injury induced by lipopolysaccharide in mice via p38MAPK and NF-κB signal pathways, Int. Immunopharm. 26 (2015) 229–236.
[15] T. Qin, D. Feng, B. Zhou, L. Bai, S. Zhou, J. Du, G. Xu, Y. Yin, Melatonin attenuates lipopolysaccharide-induced immune dysfunction in dendritic cells, Int. Immunopharm. 120 (2023), 110282.
[16] Z. Li, L. Song, L.Y. Chen, N. Zhao, J. Li, A Whole Blood Proteomics Analysis Method, 2022, CN：CN115541888A.
[17] M.P. Molloy, C. Hill, M.B. O'Rourke, J. Chandra, P. Steffen, M.J. McKay, D. Pascovici, B.R. Herbert, Proteomic analysis of whole blood using volumetric absorptive microsampling for precision medicine biomarker studies, J. Proteome Res. 21 (2022) 1196–1203.
[18] J. Ru, P. Li, J. Wang, W. Zhou, B. Li, C. Huang, P. Li, Z. Guo, W. Tao, Y. Yang, X. Xu, Y. Li, Y. Wang, L. Yang, TCMSP: a database of systems pharmacology for drug discovery from herbal medicines, J. Cheminf. 6 (2014) 13.
[19] H.Y. Xu, Z.M. Liu, Y. Fu, Y.Q. Zhang, J.J. Yu, F.F. Guo, S.H. Tang, C.Y. Lv, J. Su, R.Y. Cui, H.J. Yang, [Exploiture and application of an internet-based computation platform for integrative pharmacology of traditional Chinese medicine], Zhongguo Zhong Yao Za Zhi. 42 (2017) 3633–3638.
[20] J. Hou, X. Zhou, P. Wang, C. Zhao, Y. Qin, F. Liu, L. Yu, H. Xu, An integrative pharmacology-based approach for evaluating the potential effects of purslane seed in diabetes mellitus treatment using UHPLC-LTQ-orbitrap and TCMIP V2.0, Front. Pharmacol. 11 (2020), 593693.
[21] R. Yuan, Y. Li, S. Han, X. Chen, J. Chen, J. He, H. Gao, Y. Yang, S. Yang, Y. Yang, Fe-curcumin nanozyme-mediated reactive oxygen species scavenging and anti-inflammation for acute lung injury, ACS Cent. Sci. 8 (2022) 10–21.
[22] J. Xie, H. Wang, Y. Kang, L. Zhou, Z. Liu, B. Qin, X. Ma, X. Cao, D. Chen, W. Lu, C. Yao, K. Yu, X. Yao, H. Shang, H. Qiu, Y. Yang, The epidemiology of sepsis in Chinese ICUs: a national cross-sectional survey, Crit. Care Med. 48 (2020) e209–e218.
[23] D. Jarczak, A. Nierhaus, Cytokine storm-definition, causes, and implications, Int. J. Mol. Sci. 23 (2022).
[24] H. Jin, Z. Zhao, Q. Lan, H. Zhou, Z. Mai, Y. Wang, X. Ding, W. Zhang, J. Pi, C.E. Evans, X. Liu, Nasal delivery of hesperidin/chitosan nanoparticles suppresses cytokine storm syndrome in a mouse model of acute lung injury, Front. Pharmacol. 11 (2020), 592238.
[25] B. Al-Ani, A.M. ShamsEldeen, S.S. Kamar, M.A. Haidara, F. Al-Hashem, M.Y. Alshahrani, A.M. Al-Hakami, D.H.A. Kader, A. Maarouf, Lipopolysaccharide induces acute lung injury and alveolar haemorrhage in association with the cytokine storm, coagulopathy and AT1R/JAK/STAT augmentation in a rat model that mimics moderate and severe Covid-19 pathology, Clin. Exp. Pharmacol. Physiol. 49 (2022) 483–491.
[26] C. Pelaia, C. Tinello, A. Vatrella, G. De Sarro, G. Pelaia, Lung under attack by COVID-19-induced cytokine storm: pathogenic mechanisms and therapeutic implications, Ther. Adv. Respir. Dis. 14 (2020), 1753466620933508.
[27] X.J. Shi, Q. Jin, Y. Zhao, M.C. Xu, H. Zhang, H.D. Sheng, Y. Wang, X.P. Zhao, [Effects of Angong Niuhuang Pills against heart failure based on cross-scale polypharmacological study], Zhongguo Zhong Yao Za Zhi. 47 (2022) 1888–1896.
[28] W.J. Fu, T. Lei, Z. Yin, J.H. Pan, Y.S. Chai, X.Y. Xu, Y.X. Yan, Z.H. Wang, J. Ke, G. Wu, R.H. Xu, M. Paranjpe, L. Qu, H. Nie, Anti-atherosclerosis and cardio-protective effects of the Angong Niuhuang Pill on a high fat and vitamin D3 induced rodent model of atherosclerosis, J. Ethnopharmacol. 195 (2017) 118–126.
[29] A.M. Hamilton, J.T. Lambert, L.K. Parajuli, O. Vivas, D.K. Park, I.S. Stein, J.N. Jahncke, M.E. Greenberg, S.S. Margolis, K. Zito, A dual role for the RhoGEF Ephexin5 in regulation of dendritic spine outgrowth, Mol Cell Neurosci. 80 (2017) 66–74.
[30] B. Tsoi, X. Chen, C. Gao, S. Wang, S.C. Yuen, D. Yang, J. Shen, Neuroprotective effects and hepatorenal toxicity of angong Niuhuang wan against ischemia-reperfusion brain injury in rats, Front. Pharmacol. 10 (2019) 593.
[31] D.I. Kim, S.R. Kim, H.J. Kim, S.J. Lee, H.B. Lee, S.J. Park, M.J. Im, Y.C. Lee, PI3K-γ inhibition ameliorates acute lung injury through regulation of IκBα/NF-κB pathway and innate immune responses, J. Clin. Immunol. 32 (2012) 340–351.
[32] Y.W. Wang, Y.H. Wu, J.Z. Zhang, J.H. Tang, R.P. Fan, F. Li, B.Y. Yu, J.P. Kou, Y.Y. Zhang, Ruscogenin attenuates particulate matter-induced acute lung injury in mice via protecting pulmonary endothelial barrier and inhibiting TLR4 signaling pathway, Acta Pharmacol. Sin. 42 (2021) 726–734.
[33] S.B. Shaikh, Y. Prabhakar Bhandary, Effect of curcumin on IL-17A mediated pulmonary AMPK kinase/cyclooxygenase-2 expressions via activation of NFκB in bleomycin-induced acute lung injury in vivo, Int. Immunopharm. 85 (2020), 106676.
[34] X. Meng, L. Hu, W. Li, Baicalin ameliorates lipopolysaccharide-induced acute lung injury in mice by suppressing oxidative stress and inflammation via the activation of the Nrf2-mediated HO-1 signaling pathway, N. Schmied. Arch. Pharmacol. 392 (2019) 1421–1433.
[35] Y. Long, Y. Xiang, S. Liu, Y. Zhang, J. Wan, Q. Yang, M. Cui, Z. Ci, N. Li, W. Peng, Baicalin liposome alleviates lipopolysaccharide-induced acute lung injury in mice via inhibiting TLR4/JNK/ERK/NF-κB pathway, Mediat. Inflamm. 2020 (2020), 8414062.
[36] Y. Feng, B. Zhu, Y. Liu, Y. Liu, G. Zhou, L. Yang, L. Liu, J. Ren, Y. Hou, H. Yu, P. Meng, Y. Jiang, X. Wang, Yindan Jiedu granules exhibit anti-inflammatory effect in patients with novel Coronavirus disease (COVID-19) by suppressing the NF-κB signaling pathway, Phytomedicine. 95 (2022), 153784.
[37] X. Chen, X. Yang, T. Liu, M. Guan, X. Feng, W. Dong, X. Chu, J. Liu, X. Tian, X. Ci, H. Li, J. Wei, Y. Deng, X. Deng, G. Chi, Z. Sun, Kaempferol regulates MAPKs and NF-κB signaling pathways to attenuate LPS-induced acute lung injury in mice, Int. Immunopharm. 14 (2012) 209–216.
[38] R. Yang, L. Yang, X. Shen, W. Cheng, B. Zhao, K.H. Ali, Z. Qian, H. Ji, Suppression of NF-κB pathway by crocetin contributes to attenuation of lipopolysaccharide-induced acute lung injury in mice, Eur. J. Pharmacol. 674 (2012) 391–396.